Annual Review of Chaos Theory, Bifurcations and Dynamical Systems
Vol. 7, (2017) 1-21, www.arctbds.com.

Dynamical behavior of Peter-De-Jong map using the modified 0-1 and 3ST tests for chaos

Thierry Tanze Wontchui
Department of Physics, Faculty of Science, University of Ngaoundéré, Cameroon
e-mail: thierrywontchui@gmail.com

Joseph Yves Effa
Department of Physics, Faculty of Science, University of Ngaoundéré, Cameroon
e-mail: yveseffa@gmail.com

Henri Paul Ekobena Fouda
Laboratoire d'Analyses, Simulations et Essais, IUT, University of Ngaoundéré, Cameroon
e-mail: hekobena@gmail.com

Jean Sire Armand Eyebe Fouda
Department of Physics, Faculty of Science, University of Yaoundé 1, Cameroon
e-mail: efoudajsa@yahoo.fr

Abstract: In this paper, a detailed analysis of the behavior of Peter-De-Jong map using the modified 0-1 and 3ST tests is presented. The results show that both tests work well and effectively distinguish chaotic and regular motions in all the studied cases. The simulation times necessary in all the cases are largely inferior to the ones obtained using the 0-1 test which requires long data sets to perform well. We also performed some comparisons between the 0-1 test and the 3ST test for the litigious cases for which the decision by the 0-1 method is ambiguous, and we claim that the 3ST test can be a good alternative to the 0-1 method. The 3ST test is a very efficient method and is particularly useful in characterizing the quasi-periodic motion.

Keywords: Chaos, 0-1 test, Modified 0-1 test, 3ST test, Peter-De-Jong map.

Manuscript accepted January 20, 2017.

1 Introduction

With the discovery of chaos phenomenon in 1963 by Edward Lorenz [19], the field of nonlinear dynamics has attracted much attention of researchers around the world, leading thus to numerous publications [17, 1]. This phenomenon, owing to its remarkable properties such as ergodicity, extreme sensitivity to initial conditions and control parameters of system, etc. [17, 23], is applying to diverse areas of science as electronic, biology, secure communication, economy, meteorology, etc. Therefore, the determination of regular or chaotic nature of dynamical systems becomes crucial.

Many tools to characterize chaos in these systems have been proposed since long time [1, 2, 9, 14]. We can sort them in two categories: the qualitative methods and quantitative methods. As qualitative method, we can quote: the phase portrait and the bifurcation diagram. This latter is obtained by representing the states of system when one of the control parameters varies. These two techniques just allow us to have a certain idea on the behavior of the system, and are based on visual perception that can prove to be wrong. As quantitative method, we have: the SALI method (Small Alignment Index) [21], the Largest Lyapunov Exponent [24], Entropy [13], the Fast Lyapunov Indicator [8], the Dynamic Lyapunov Indicator [25], the Delay Vector Variance method [15], and so on. However, most of these techniques exhibit practical limitations since they fail to detect chaos for a large class of dynamical systems (non-universality of the tests), require the absolute knowledge of mathematical equations governing the dynamics of the systems (impossibility to handle the experimental data), require a large amount of data which is expensive in computational time, fail to analyze the time series contaminated by noise, complexity of test algorithm, etc. Despite of a lot of efforts devoted, one of the major challenges in the field of characterization of nonlinear dynamical systems remains to propose a test that can overcomes all these limitations.

In a recent past, a new test allowing detection of regular or chaotic nature in deterministic dynamical systems has been proposed by Gottwald and Melbourne, the 0-1 test [10, 12]. It is a binary test which takes in input, the time series data of the deterministic dynamical system and returns 0 or 1 according that the dynamics is respectively regular or chaotic. It does not require the prior knowledge of mathematical equations governing the dynamics of system and the phase space reconstruction which is quite complex [12]. In addition, it is robust to the presence of noise and it is easy to implement. The 0-1 test has been successfully applied to diverse type of system [20, 22, 4, 5, 18] and its reliability has been proved [16, 11]. However, the main disadvantages of this test are: it requires a large amount of data to perform well and its algorithm is based on computing of several multiplications and integrals which are expensive in computation time; it equally fails to detect the nature of the systems when the data are oversampled; the 0-1 test does not also allows distinction between periodic and quasi-periodic behaviors.

In order to overcome the drawbacks of the 0-1 test, two other new tests have recently been proposed by Fouda and his coworkers. These tests are: the modified 0-1 test [6]

and the Three-State test (3ST) [7]. Their reliability should be support by testing them on large and different classes of dynamical systems. In this paper, these two methods are clearly presented and extended to time series data generated by Peter-De-Jong map. We use here this kind of map because it exhibits several complex types of attractors for different set of parameters. The rest of paper is structured as follows: in Section 2, we briefly study the modified 0-1 test. Section 3 is devoted to a detailed study of 3ST test. The Section 4 is consecrated first to the presentation of the Peter-De-Jong map, then we apply the modified 0-1 and 3ST tests to data generated by this map. The results are shown and discussed in this section. Section 5 shows the speed performance of the modified 0-1 and 3ST tests compared to the one of 0-1 test. Finally, Section 6 includes the conclusion of this work.

2 Description of the modified 0-1 test

The modified 0-1 test [6] is a binary test that takes in input the sub-observable and returns 0 or 1 according that the dynamics is respectively regular or chaotic. Here, the sub-observable is defined by mapping exclusively the local maxima and minima (extrema) of the observable. These extrema are computed by detecting the sign changes in the first derivative of the observable. We recall that, the observable is the time series data generated by the underlying dynamical system. This modification does not change the dynamic of system. Therefore if the observable is regular, the sub-observable is also regular and if it is chaotic, the sub-observable remains chaotic. In addition of all the advantages of the traditional 0-1 test, the modified 0-1 test successfully detects chaos in oversampled data [6]. The implementation of modified 0-1 test is given below [6]:
Given an observable $\phi(j)$ with $j = 1, 2, \cdots, N$, we first define the sub-observable $\psi(k)$ with $k = 1, 2, \cdots, L < N$, which is a vector consisting by the local maxima and minima of the entire observable $\phi(j)$. Then, we compute the translations variables $p(n)$ and $q(n)$ of $\psi(k)$. They are defining as

$$p(n) = \sum_{k=1}^{n} \psi(k) \cos(kc) \tag{1}$$

and

$$q(n) = \sum_{k=1}^{n} \psi(k) \sin(kc) \tag{2}$$

where $c \in (0, \pi)$ is the sampling frequency of the time series and $n = 1, 2, \cdots, L$.
The plot of $p - q$ diagram allows us to have a certain idea on the behavior of the system. If the motion is a torus, the dynamic is regular. If it behaves like a Brownian motion, the dynamics is said to be chaotic.

The behavior of $p(n)$ and $q(n)$ can be characterized by computing the mean square displacement (MSD) defined as:

$$M(n) = \lim_{L\to\infty} \frac{1}{L} \sum_{k=1}^{L} [(p(k+n) - p(k))^2 + (q(k+n) - q(k))^2] \tag{3}$$

where $n = 1, 2, \cdots, L/10$.
In order to remove the oscillatory component of $M(n)$, the modified mean square displacement is calculated as follows [12]:

$$D(n) = M(n) - V_{osc}(n) \tag{4}$$

where

$$V_{osc}(n) = E_\psi)^2 \frac{1 - \cos(nc)}{1 - \cos(c)} \tag{5}$$

and

$$E_\psi = \lim_{L\to\infty} \frac{1}{L} \sum_{k=1}^{L} \psi(k) \tag{6}$$

V_{osc} is the oscillatory component of $M(n)$ and E_ψ the average of the sub-observable.
We will use Eq. (4) below to plot the MSD. When this latter is bounded in time, the dynamics of the system is called regular whereas if it grows linearly in time, the dynamics is said to be chaotic.
Finally, we compute the asymptotic growth rate K_c of the MSD on which the test is based. There are two methods to calculate K_c: the regression method and the correlation method. We will use the second method since it allows a better convergence of the asymptotic growth rate. It is given by:

$$K_c = \frac{cov(\xi, \Delta)}{\sqrt{var(\xi)var(\Delta)}} \tag{7}$$

where $\xi = 1, 2, \cdots, L/10$ and $\Delta = D(1), D(2), \cdots, D(L/10)$ are the vectors.
However for some isolated values of c (resonances values), the test fails to detect the dynamics of system. To avoid that, K_c is computed for N_c values of c for a same parameter value ($N_c = 100$, is sufficient in practice); the final asymptotic growth rate K is computed as the median of N_c values of K_c. If $K_c \approx 0$, the dynamics of the system is said to be regular whereas if $K_c \approx 1$ it is known as chaotic.

Despite of the improvement of the 0-1 test, the modified 0-1 test does not allow to distinguish between periodic and quasi-periodic motions. In order to overcome this limitation, another test for chaos detection in discrete dynamical systems has been proposed; it is the 3ST test.

3 Description of the three state test (3ST)

The 3ST test [7] is another technique that allows chaos detection in discrete dynamical systems. It is based on the pattern analysis of data series. It studies the distribution of the system states in a data series as a function of time. The 3ST considers the properties of periodic and quasi-periodic signal for determining whether the dynamics of a system is regular or chaotic [7]. In addition to the afore-mentioned advantages of the 0-1 test, the 3ST test has been developed to make a clear distinction between periodic, quasi-periodic and chaotic behaviors; it has also been developed for real time application due to the fact that its implementation most use addition and subtraction operators; and finally for automating the detection of the period doubling route to chaos. The implementation of 3ST test is shown below [7]:
given an observable to be characterized $x_j(k) = \Phi(x(k))$ with $k \in \mathbb{N}$, $x(k) = (x_1, x_2, \cdots, x_M)(k)$ the state vector, $1 \leq j \leq M$; for determining its patterns, we define $u_j = g(x_j)$ which is the time series data sorted by ascending order with g a function; then we also define $v_j = q(u_j) = q(g(x_j))$ representing the distribution of indices outputting the initial positions of the values of u_j in x_j.
In order to take into account the time dependence of $v_j(k, N)$ (N being the length of time series data), the largest slope (LS) is defined as pattern characteristic as follows:

$$LS(n) = \max_{1 \leq k \leq N-1} (v_j(k+1, N) - v_j(k, N)) \tag{8}$$

It is then possible to use its mean square error $\sigma_{LS}(N, n)$ for chaos detection in time series data as follows:

$$\sigma_{LS}(N, n) = \sqrt{\frac{1}{N} \sum_{j=0}^{p} (LS(jN_0 + n) - \overline{LS})^2} \tag{9}$$

with

$$\overline{LS} = \frac{1}{N} \sum_{j=1}^{p} LS(jN_0 + n) \tag{10}$$

where $N = pN_0 + n$ is the length of data series, N_0 the integration step and p a natural number different from zero. $\sigma_{LS}(N, n)$ measures the ability of a dynamical system to generate new patterns as the time is increasing. n is the smallest observation duration for the LS to be well evaluated and should verify the relation $n \ll N$. According to the behavior of LS, $\sigma_{LS}(N, n)$ is bounded if the underlying dynamics is non chaotic. For this purpose, we define

$$\mu(N, n) = \frac{\log(1 + \sigma_{LS}(N, n))}{\log N} \tag{11}$$

then

$$K(n) = \lim_{n \to +\infty} \mu(N, n) \tag{12}$$

K is the asymptotic growth rate of the mean square error of LS. K is equal to zero in the case of periodic and quasi-periodic motions and greater than zero in the case of chaotic motion.

In order to distinguish periodic from quasi-periodic motions, the global derivative of $\mu(N, n)$ is computed. Its sign can then allow distinguishing these two behaviors. This global derivative is defined as:

$$\lambda(n) = \lim_{n \to +\infty} \sum_{k=1}^{m-1} (\mu(N_{k+1}, n) - \mu(N_k, n)) \tag{13}$$

where $N_1 \ll N_m$. N_1 is the smallest integration duration and N_m is the greatest one. In practice, choose the time delay $n \leq N_1/2$ leads to good results. λ is the periodicity index and allows characterizing regular and chaotic dynamics. The 3ST test is based on its sign: $\lambda(n) < 0$ for quasi-periodic behavior, $\lambda(n) = 0$ for periodic behavior and $\lambda(n) > 0$ for chaotic behavior. Thus, the 3ST as indicated by its name allows to have in output three main parameters which are: L the cycle of periodic orbits, K the asymptotic growth rate of the largest slope and λ the periodicity index.

Moreover, 3ST like other chaos detection tools is extremely sensitive to small change in the input time series. To make it more robust to the presence of noise, an absolute threshold α has been introduced on the input time series such that two states $\tilde{x}(k)$ and $\tilde{x}(j)$ are assumed to be different if and only if $|\tilde{x}(k) - \tilde{x}(j)| \geq \alpha$. The effectiveness of the studied tests is shown by applying them to time series data generated from the Peter-De-Jong map.

4 Peter-De-Jong map: Application of the modified 0-1 and 3ST tests

The Peter-De-Jong map is a pair of difference equations suggested by Peter-De-Jong and so named after him [3]. It is a chaotic system that appears simple, but exhibiting several complex types of attractors, corresponding to different sets of parameters. The map is described as:

$$\begin{cases} x_{n+1} &= \sin(ay_n) - \cos(bx_n) \\ y_{n+1} &= \sin(cx_n) - \cos(dy_n) \end{cases} \tag{14}$$

where a, b, c and d are the parameters of the system.
Below, different sets of these parameters are presented. For each set, we evolved the map (Eq. (14)) and analyzed the obtained time series data through the modified 0-1 and 3ST tests. The results are compared to those of the ordinary 0-1 test and phase portrait plot as shown in Fig. 1 to Fig. 10 below. Also, the values of K by 0-1 test, K_{mod} by modified 0-1 test, K_{3ST} and λ for 3ST are given for each set of parameters. We used an input

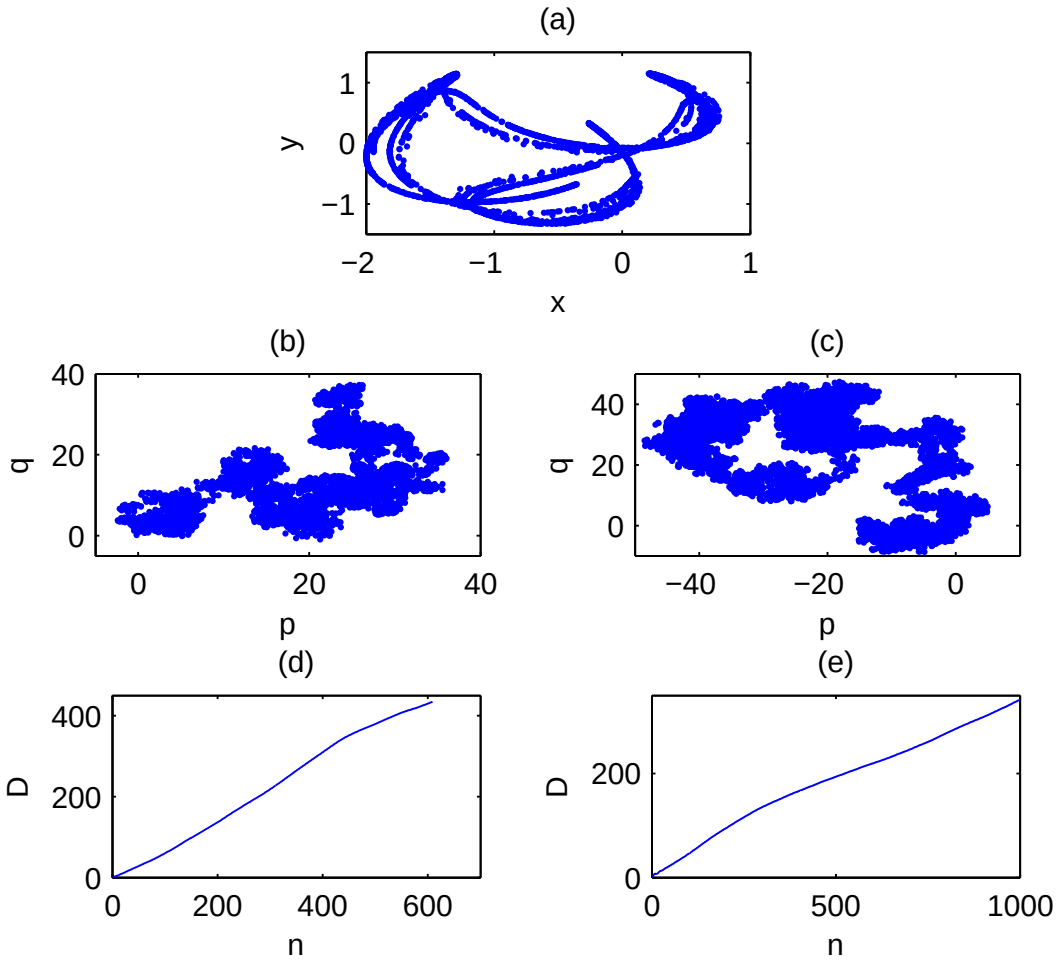

Figure 1: Plot of (a) phase portrait, (b) p-q diagram for the modified 0-1 test, (c) p-q diagram for the 0-1 test, (d) mean square displacement for the modified 0-1 test and (e) mean square displacement for the 0-1 test. The parameter values are: $a = 2.033372$, $b = -0.78980076$, $c = -0.5964787$, $d = -1.7829015$. $K = 0.9974$; $K_{mod} = 0.9988$; $K_{3ST} = 0.8225$; $\lambda = 0.0983$.

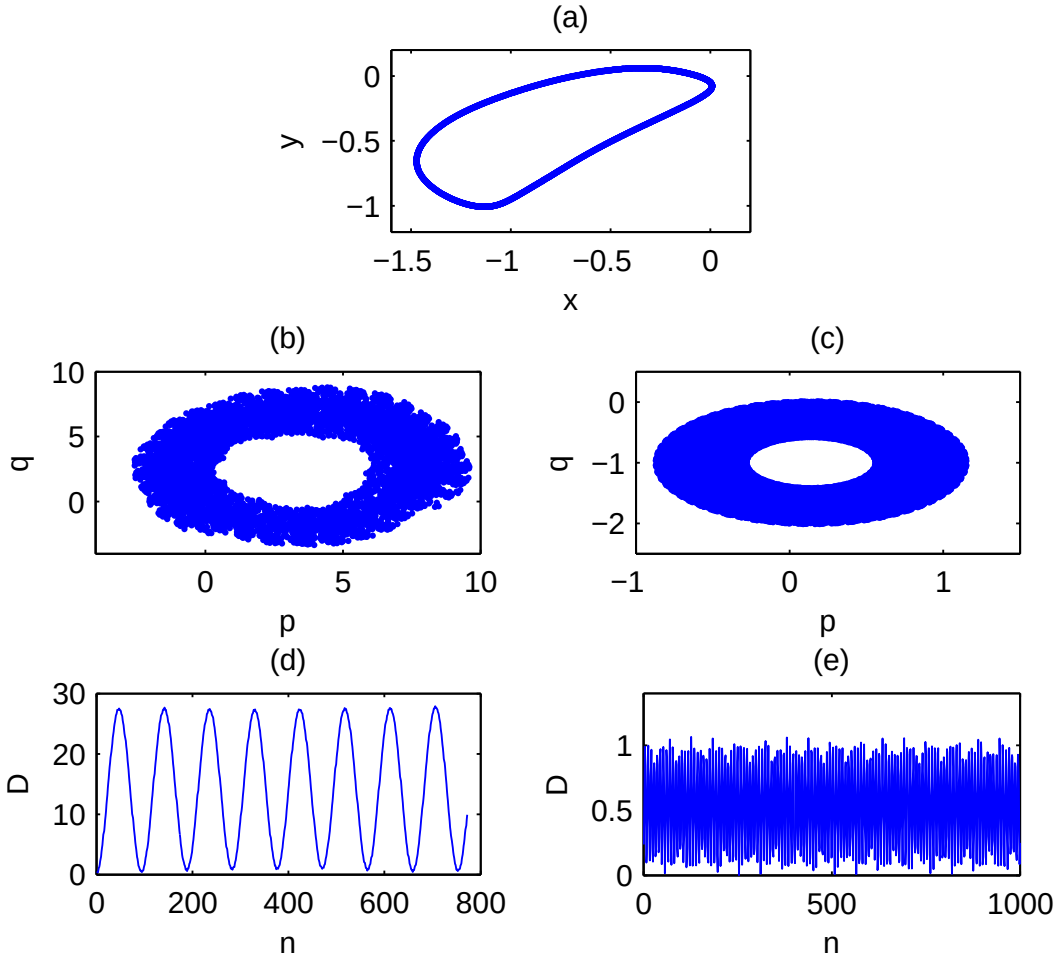

Figure 2: Plot of (a) phase portrait, (b) p-q diagram for the modified 0-1 test, (c) p-q diagram for the 0-1 test, (d) mean square displacement for the modified 0-1 test and (e) mean square displacement for the 0-1 test. The parameter values are: $a = 1.76$, $b = 1.66571$, $c = -0.86114$, $d = 0.59714$. $K = -0.0055$; $K_{mod} = -0.0668$; $K_{3ST} = 0.4537$; $\lambda = -0.0617$.

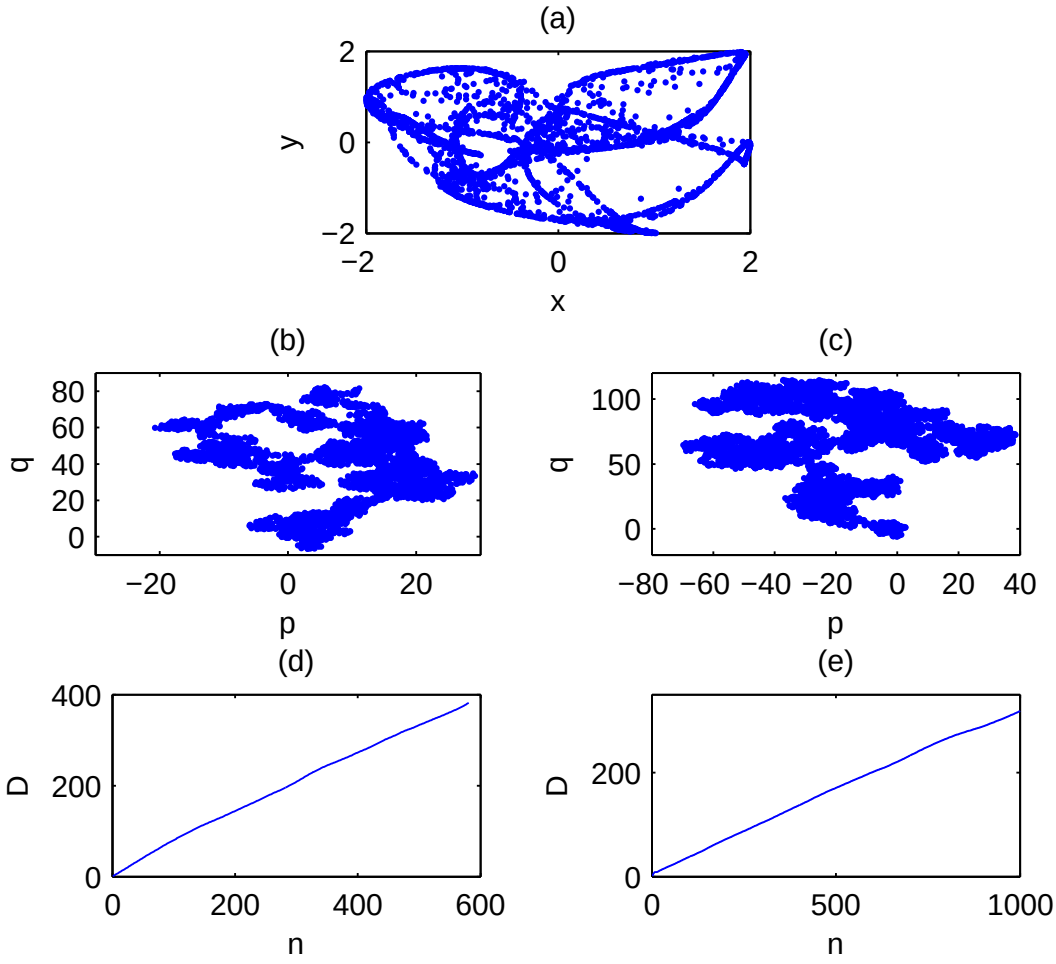

Figure 3: Plot of (a) phase portrait, (b) p-q diagram for the modified 0-1 test, (c) p-q diagram for the 0-1 test, (d) mean square displacement for the modified 0-1 test and (e) mean square displacement for the 0-1 test. The parameter values are: $a = 0.973894$, $b = 1.66504$, $c = -0.860796$, $d = 2.10487$. $K = 0.9937$; $K_{mod} = 0.9991$; $K_{3ST} = 0.8211$; $\lambda = 0.1015$.

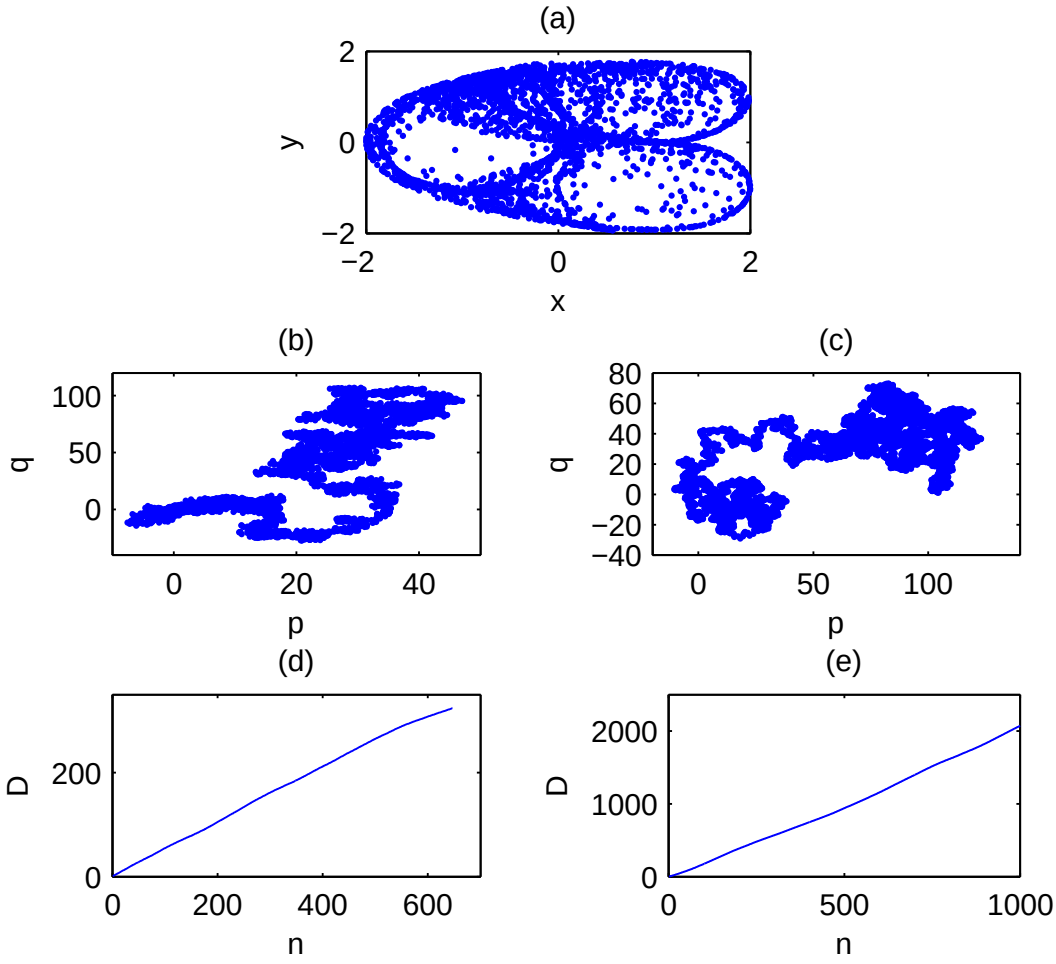

Figure 4: Plot of (a) phase portrait, (b) p-q diagram for the modified 0-1 test, (c) p-q diagram for the 0-1 test, (d) mean square displacement for the modified 0-1 test and (e) mean square displacement for the 0-1 test. The parameter values are: $a = 2.07345$, $b = 1.66504$, $c = -0.860796$, $d = 2.10487$. $K = 0.9996$; $K_{mod} = 0.9905$; $K_{3ST} = 0.8263$; $\lambda = 0.0953$.

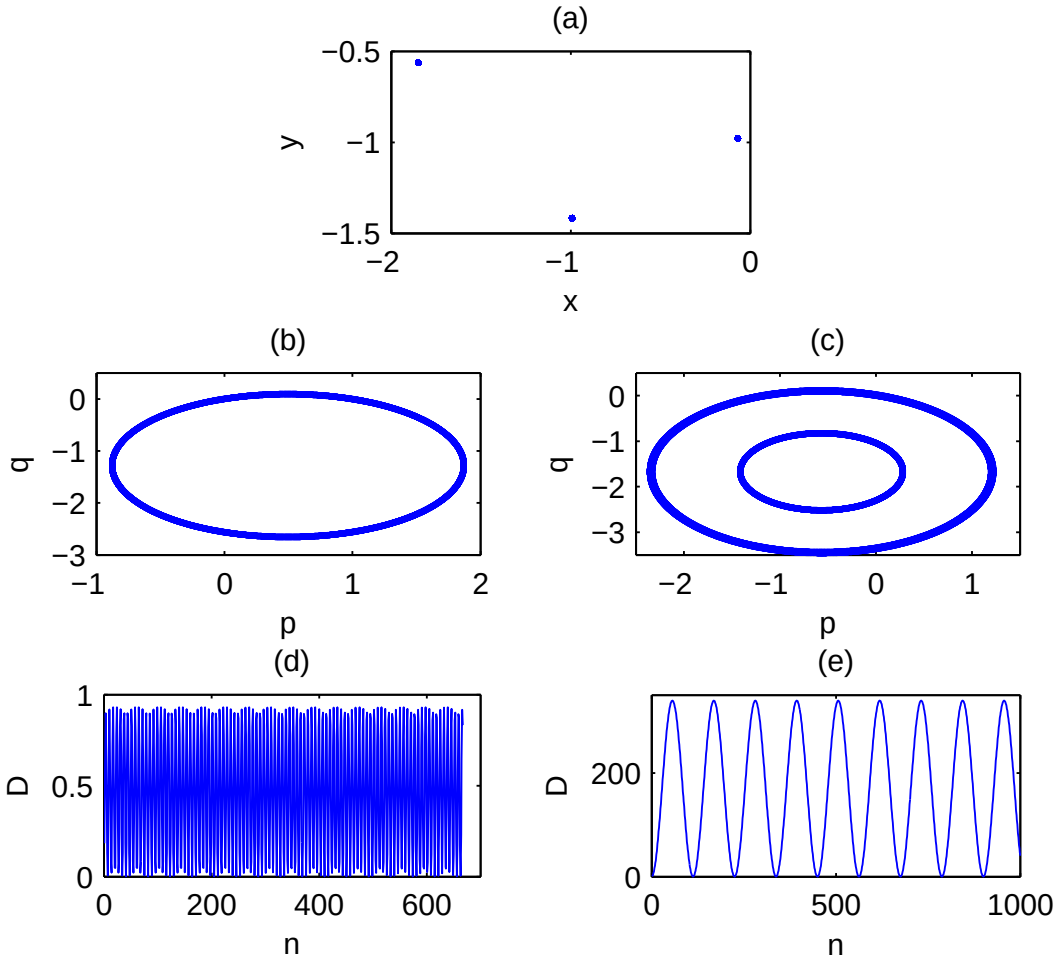

Figure 5: Plot of (a) phase portrait, (b) p-q diagram for the modified 0-1 test, (c) p-q diagram for the 0-1 test, (d) mean square displacement for the modified 0-1 test and (e) mean square displacement for the 0-1 test. The parameter values are: $a = 1.07345$, $b = 2.785398$, $c = 1.34786$, $d = 1.10487$. $K = -0.0033$; $K_{mod} = -0.00015$; $K_{3ST} = 0$; $\lambda = 0$.

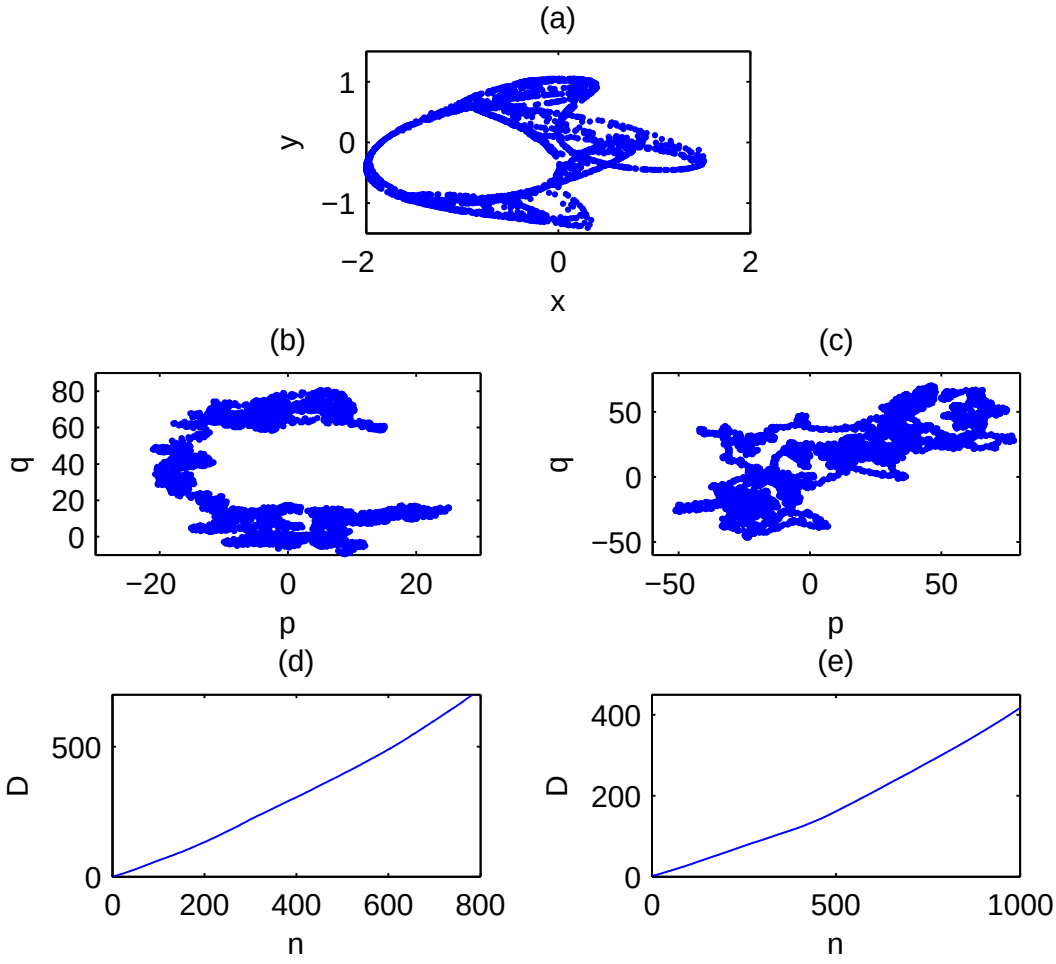

Figure 6: Plot of (a) phase portrait, (b) p-q diagram for the modified 0-1 test, (c) p-q diagram for the 0-1 test, (d) mean square displacement for the modified 0-1 test and (e) mean square displacement for the 0-1 test. The parameter values are: $a = 2.89027$, $b = 1.5708$, $c = -0.314159$, $d = 2.10487$. $K = 0.9950$; $K_{mod} = 0.9821$; $K_{3ST} = 0.8241$; $\lambda = 0.0966$.

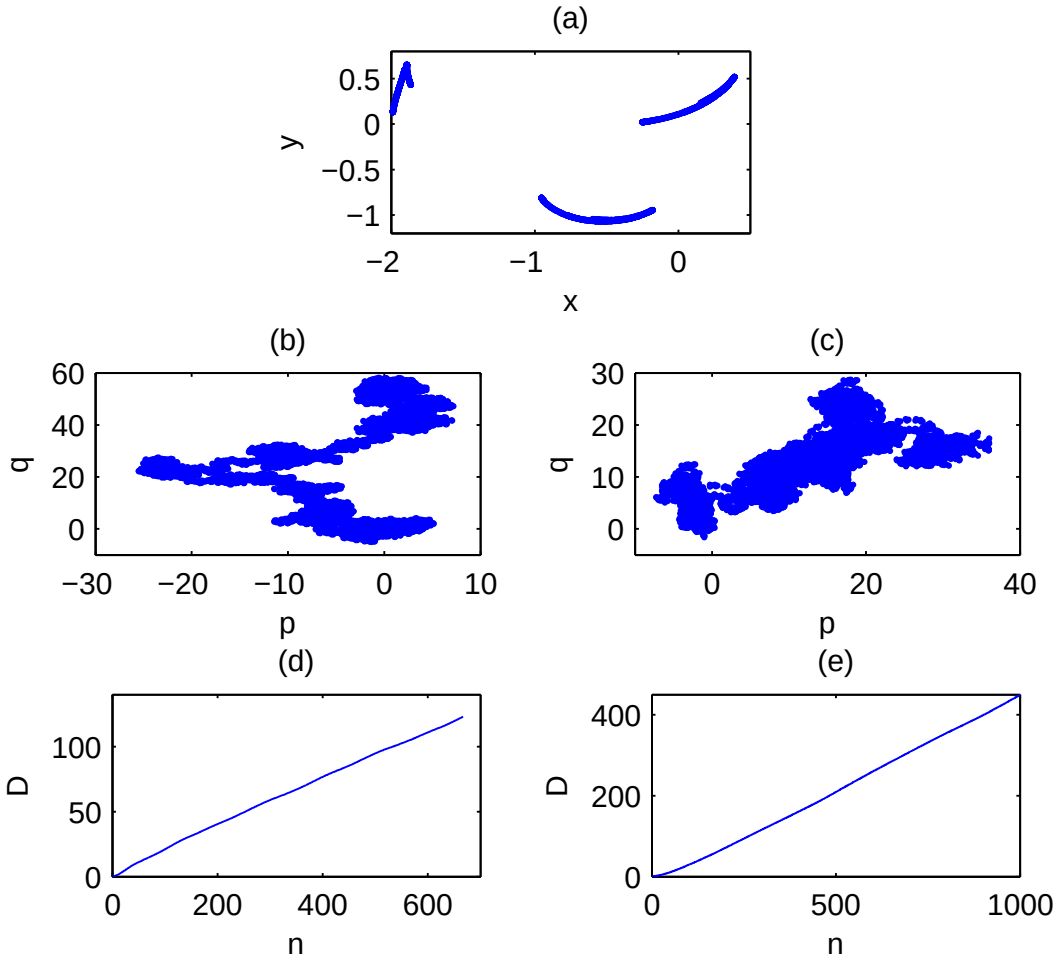

Figure 7: Plot of (a) phase portrait, (b) p-q diagram for the modified 0-1 test, (c) p-q diagram for the 0-1 test, (d) mean square displacement for the modified 0-1 test and (e) mean square displacement for the 0-1 test. The parameter values are: $a = 1.7843$, $b = 0.5366543$, $c = -0.7553879$, $d = 1.65469$. $K = 0.8975$; $K_{mod} = 0.9872$; $K_{3ST} = 0.8164$; $\lambda = 0.0911$.

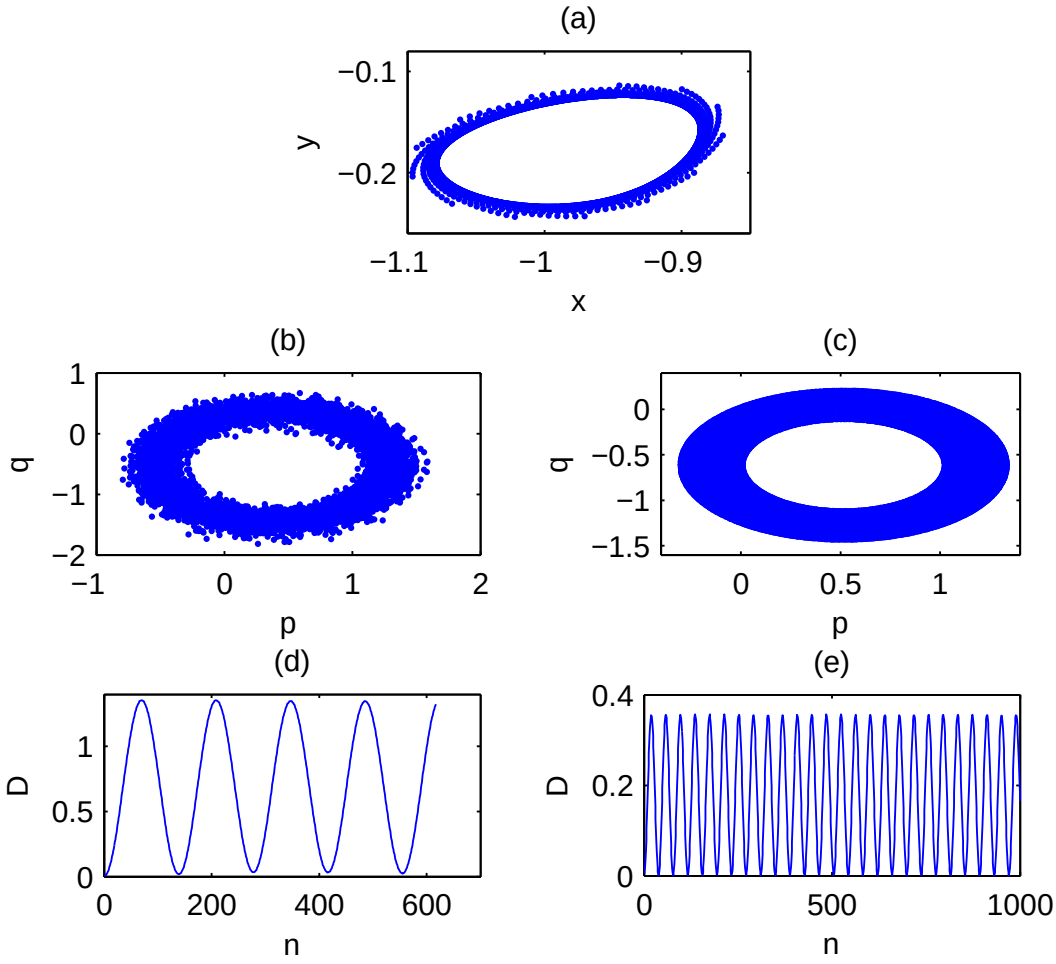

Figure 8: Plot of (a) phase portrait, (b) p-q diagram for the modified 0-1 test, (c) p-q diagram for the 0-1 test, (d) mean square displacement for the modified 0-1 test and (e) mean square displacement for the 0-1 test. The parameter values are: $a = 1.7843$, $b = 0.8574$, $c = -0.975840$, $d = 0.65469$. $K = -0.0011$; $K_{mod} = 0.0092$; $K_{3ST} = 0$; $\lambda = 0$.

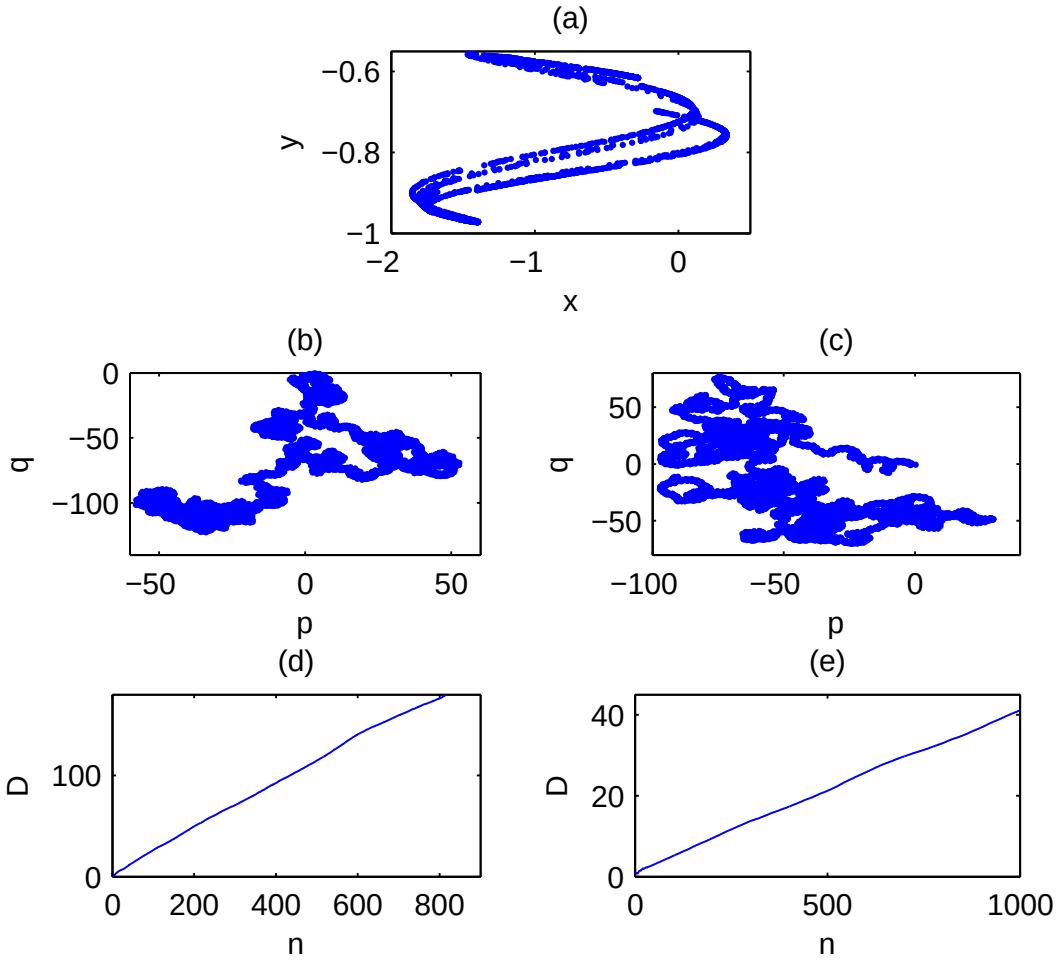

Figure 9: Plot of (a) phase portrait, (b) p-q diagram for the modified 0-1 test, (c) p-q diagram for the 0-1 test, (d) mean square displacement for the modified 0-1 test and (e) mean square displacement for the 0-1 test. The parameter values are: $a = 1.273574$, $b = 2.8574$, $c = -0.175345$, $d = 0.55469$. $K = 0.9972$; $K_{mod} = 0.9962$; $K_{3ST} = 0.8241$; $\lambda = 0.0770$.

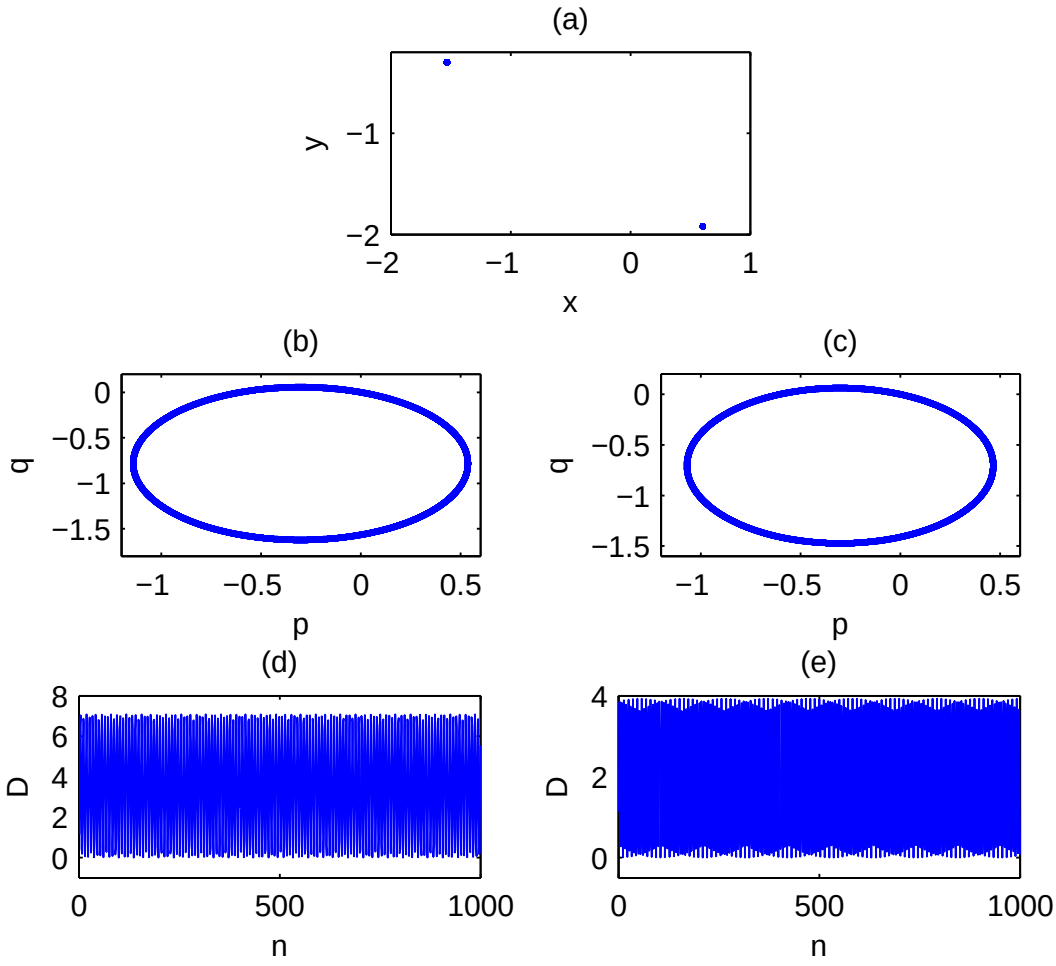

Figure 10: Plot of (a) phase portrait, (b) p-q diagram for the modified 0-1 test, (c) p-q diagram for the 0-1 test, (d) mean square displacement for the modified 0-1 test and (e) mean square displacement for the 0-1 test. The parameter values are: $a = 0.76453$, $b = 1.66571$, $c = 1.28857$, $d = 0$. $K = 0.00042$; $K_{mod} = -0.00058$; $K_{3ST} = 0$; $\lambda = 0$.

sequence of length $N = 2000$ for the 3ST algorithm and $N = 10000$ for the 0-1 and the modified 0-1 tests.

The results show that for the cases of Fig. 1, Fig. 3, Fig. 4 and Fig. 6, the phase portrait plot seems to be chaotic (Fig. 1(a), Fig. 3(a), Fig. 4(a), Fig. 6(a)). This chaotic nature is confirmed by the Brownian motion of the p-q diagrams (Fig. 1(b),(c); Fig. 3(b),(c); Fig. 4(b),(c); Fig. 6(b),(c)), the linear growth of the MSD (Fig. 1(d),(e); Fig. 3(d),(e); Fig. 4(d),(e); Fig. 6(d),(e)), the parameters values K_{mod} and K_{0-1} which are approximately 1 for the modified 0-1 test and the 0-1 test as presented on these Figures. Besides, the parameters values K_{3ST} and λ_{3ST} by 3ST are greater than 0.

For the cases of Fig. 5, Fig. 8 and Fig. 10, the phase plot appears to be regular (Fig. 5(a), Fig. 8(a), Fig. 10(a)). This regular nature is confirmed by the torus motion of the p-q diagrams (Fig. 5(b),(c); Fig. 8(b),(c); Fig. 10(b),(c)), the bounded behavior of the MSD (Fig. 5(d),(e); Fig. 8(d),(e); Fig. 10(d),(e)), the parameters values K_{mod} and K_{0-1} that are close to 0 for the modified 0-1 test and 0-1 test. Also, the parameters values K_{3ST} and λ_{3ST} by 3ST are equal to 0.

In regard to the Fig. 7 and Fig. 9, the phase portrait plot does not appears to be chaotic while the modified 0-1 test, the 0-1 test and the 3ST detect chaos for these parameters. So for these cases, the phase portrait fails to detect chaos. We can explain by the fact that it is based on the visual perception which can be wrong; also, the chaos presented by the map for these parameters may be weak.

For the case of Fig. 2, the phase portrait plot seems to be regular; this regular nature is also detected by the modified 0-1 and 0-1 tests. However both tests indicate the periodic motion. The 3ST being less sensitive to the sequence of input times series generated by the system, the value of the periodicity index is $\lambda_{3ST} = -0.0617$, which may be interpreted as quasi-periodic motion. This test is a very efficient method and is particularly useful in characterizing the quasi-periodic motion.

To better characterize the behavior of the Peter-De-Jong map when a control parameter varies with the time, its global dynamics is valued using the modified 0-1 and 3ST tests for parameter value a varying from -5 to 5, with $b = -0.78980076$, $c = -0.5964787$ and $d = -1.7829015$. The results are compared with those of the 0-1 test and the bifurcation diagram as displayed in Fig. 11 below. As shown in Fig. 11, the results of the modified 0-1 and 3ST tests are in good agreement with those of the bifurcation diagram and the 0-1 test for most part of points in the range of variation of the control parameter. Nevertheless in some short ranges at $a \approx [-4, -3.8]$ and $a \approx [1, 1.2]$, the dynamics seem to be litigious. It is difficult to take a decision regarding the dynamics of the system by only visualizing the bifurcation diagram (Fig. 11(a)). The dynamics there might be quasi-periodic or weakly chaotic. In these small ranges the 0-1 test detects a regular dynamics (Fig. 11(b)) while the modified behaves as a weak chaos (Fig. 11(c)). The 3ST detects quasi-periodicity in some points of these ranges (Fig. 11(e)).

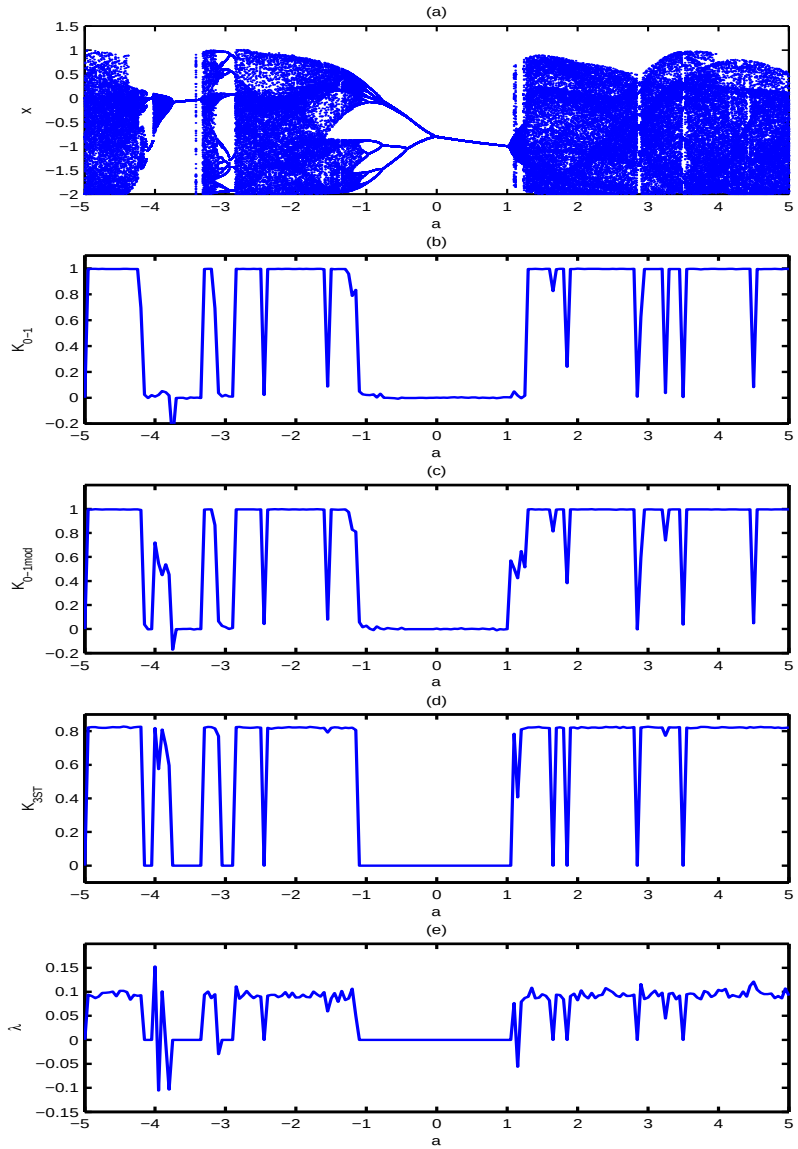

Figure 11: Global dynamics of the Peter-De-Jong map for control parameter a varying from -5 to 5: (a) bifurcation diagram, (b) asymptotic growth rate K_{0-1} by 0-1 test, (c) asymptotic growth rate K_{mod} by modified 0-1 test, (d) asymptotic growth rate K_{3ST} by 3ST test and (e) periodicity index λ_{3ST} by 3ST test.

5 Speeds analysis

For an efficient using of chaos detection methods for applications in areas of science, we must be able to process the data in real time. For this purpose, we propose to compare the processing speeds of the above studied tests for chaos detection. All the operations are implemented using Matlab 7.9.0 (R2009b) on a personal computer equipped with an Intel(R) Core(TM) i3-M370, 2.40 GHz CPU, running Windows 7.

In regard to the cases 1 to 10 (Fig. 1 to Fig. 10), the average simulation time for each case is around $35s$ for the modified 0-1 test; $84s$ for the 0-1 test and $0.1s$ for the 3ST test. We notice that the computation time of the modified 0-1 test is 2.4 times lower than the one of the 0-1 test and 350 times greater than the one of the 3ST test. So the simulation time of the 3ST test is quite inconsiderable compared to those of others tests. The simulation time of the modified 0-1 test is significantly reduced since the number of data to be processed is reduced. For example, if the time series to analyze is a sinusoid, we just process its maximum and minimum instead to process all points of the sinusoid. Nevertheless, despite of fact that the computation time of the modified 0-1 test compared to ordinary 0-1 test is considerably reduced, this time remains again heavy.

For the simulation time of global dynamics of the Peter-De-Jong map, we obtained $8064s$ approximately 2.24 hours for the modified 0-1 test and $11139s$ approximately 3.0942 hours for the 0-1 test. Although this time is reduced for the modified 0-1 test, it still remains quite large compared to the one of 3ST test that has been assessed to around $21s$. Thus the 3ST test is expected to process experimental data in real time.

6 Conclusion

Chaos detection in dynamical systems is a nontrivial problem. In order to generalize a method, it is important to prove its reliability. In this paper, a detailed study of the behavior of Peter-De-Jong map using two chaos detection methods namely the modified 0-1 and 3ST tests was performed. Regarding the modified 0-1 test, it consists to process only the local maxima and minima of time series data rather than treat the entire observable like the ordinary 0-1 test. The 3ST test is based on pattern analysis of time series data. These two tests for chaos do not require the knowledge of the mathematical equations governing the dynamics of system to be applied as well as the nature and the dimension of the underlying vector field. To show the effectiveness and the reliability of these tests, we must applied them to data generated by various dynamical systems. Therefore, in this work we have applied them to time series generated from the Peter-De-Jong map. The results showed that the modified 0-1 and 3ST tests perform well for all cases of parameters. These two tests for chaos have then shown their applicability to this kind of map. The paper also shows that the 3ST test can be a better alternative to 0-1 test and classical methods as it detects quasi-periodic motion in the map where the others tests fail. Based on the time that has allowed us to simulate the global dynamics of the

Peter-De-Jong map, we can say that the 3ST can be used to process experimental data in real time. In prospect, we plane to apply the 3ST test to real world data.

References

[1] M. Barahona and C.-S. Poon. Detection of nonlinear dynamics in short, noisy time series. *Nature*, 3(81):215–217, 1996.

[2] S. Basu and E. Foufoula-Georgiou. Detection of nonlinearity and chaoticity in time series using the transportation distance function. *Phys. Lett. A*, 301(5-6):413–423, 2002.

[3] M. Budhraja, N. Kumar, and L. M. Saha. The 0-1 test applied to peter-de-jong map. *Int. J. Eng.Innov. Tech.*, 2(6):253–257, 2012.

[4] J. H. P. Dawes and M. C. Freeland. The '0-1 test for chaos' and strange nonchaotic attractors. `http://people.bath.ac.uk/jhpd20/publications/sna.pdf`, 2008.

[5] I. Falconer, G. A. Gottwald, I. Melbourne, and K. Wormnes. Application of the 0-1 test for chaos to experimental data. *SIAM J. Appl. Dyn.*, 6:395–402, 2005.

[6] J. S. A. E. Fouda, B. Bodo, S. L. Sabat, and J. Y. Effa. A modified 0-1 test for chaos detection in oversampled times series observations. *Int. J. Bifurc. Chaos*, 24(5):1450063, 2014.

[7] J. S. A. E. Fouda, J. Y. Effa, M. Kom, and M. Ali. The three-state test for chaos detection in discrete maps. *Appl. Soft Comput.*, 13(12):4731–4737, 2013.

[8] C. Froeschlé, E. Lega, and Gonczi R. Fast lyapunov indicators: Application to asteroidal motion. *Celest. Mech. Dyn. Astron.*, 67(1):41–62, 1997.

[9] J. F. Gemmeke, S. F. Portegies Zwart, and C. J. H. Kruip. Detecting irregular orbits in gravitational n-body simulations. *Commun. Nonlinear Sci. Numer. Simulat.*, 13(6):1157–1168, 2008.

[10] G. A. Gottwald and I. Melbourne. A new test of chaos in deterministic systems. *Proc. Roy. Soc. A*, 460:603–611, 2004.

[11] G. A. Gottwald and I. Melbourne. Comment on reliability of the 0-1 test for chaos. *Phys. Rev. E*, 77:028201, 2008.

[12] G. A. Gottwald and I. Melbourne. On the implementation of the 0 1 test for chaos. *SIAM J. Appl. Dyn. Syst.*, 8:129–145, 2008.

[13] P. Grassberger and I. Procaccia. Characterization of strange attractors. *Phys. Rev. Lett.*, 50(5):346–349, 1983.

[14] W. Heng-Dong, L. Li-Ping, and G. Jian-Xiu. An efficient method of distinguishing chaos from noise. *Chin. Phys. B*, 19(5):050505, 2010.

[15] S. Hou, Y. Li, and S. Zhao. Detecting the nonlinearity in time series from continuous dynamic systems based on delay vector variance method. *Int. J. Math. Computer Sci. Eng.*, 1(2):41–46, 2007.

[16] J. Hu, W.W. Tung, J. Gao, and Y. Cao. Reliability of the 0-1 test for chaos. *Phys. Rev. E*, 72:056207, 2005.

[17] M. S. Jakimoski and L. Kocarev. Chaos and cryptography. *IEEE Trans. Circ. Syst. I: Fund. Theory Appl.*, 48(2):163–169, 2001.

[18] G. Litak, A. Syta, and M. Wiercigroch. Identification of chaos in a cutting process by the 0-1 test. *Chaos, Solitons and Fractals*, 40:2095–2101, 2009.

[19] E. N. Lorenz. Deterministic nonperiodic flow. *J. Atmosph. Sci.*, 20(2):130–141, 1963.

[20] M. A. Maysoon and N. F. Mansour. Numerical and chaotic analysis of chuas circuit. *J. Emerging Trends Comput. Information Sci.*, 3:783–791, 2012.

[21] C. Skokos. Alignment indices: A new, simple method for determining the ordered and chaotic nature of orbits. *J. Phys. A*, 34(47):10029–10043, 2001.

[22] C. Skokos, C. Antonopoulos, T. C. Bountis, and M. N. Vrahatis. Detecting order and chaos in hamiltonian system by the sali method. *J. Phys. A*, 37:6269–6284, 2004.

[23] S. H. Strogatz. *Nonlinear Dynamics and Chaos with applications to Physics, Biology, Chemistry, and Engineering*. Perseus books publishing, 1994.

[24] A. Wolf, J. B. Swift, H. L. Swinney, and J. A. Vastano. Determining lyapunov exponents from a time series. *Physica D*, 16(3):285–317, 1985.

[25] M. Yuasa and L. M. Saha. Indicators of chaos. `https://www.google.cm/?gws_rd=cr,ssl&ei=BmxBWO6IBsm7UfX4iegJ#q=+Manabu+Yuasa+and+L.+M.+Saha+%2B+indicators+of+chaos+2007+pdf`, 2008.